Supplemental Information for: Ultrafast carrier experimental and *ab initio* dynamics in plasmonic nanoparticles

Ana M. Brown,[1] Ravishankar Sundararaman,[2] Prineha Narang,[1,2,3] Adam M. Schwartzberg,[4] William A. Goddard III,[2,5] and Harry A. Atwater[1,2]

[1] *Thomas J. Watson Laboratories of Applied Physics, California Institute of Technology*
[2] *Joint Center for Artificial Photosynthesis, California Institute of Technology*
[3] *NG NEXT, 1 Space Park Drive, Redondo Beach CA*
[4] *The Molecular Foundry, Lawrence Berkeley National Laboratory, 1 Cyclotron Road, Berkeley CA*
[5] *Materials and Process Simulation Center, California Institute of Technology, 1200 East California Blvd, Pasadena CA 91125 USA*

(Dated: December 17, 2016)

SPATIAL DYNAMICS OF ELECTRONS

As experimental systems for ultrafast spectroscopy of metals, both thin films and nanoparticles have distinct advantages and disadvantages. Thin films are in general a cleaner system, offering potentially much better control over geometry, surface quality and grain-size / crystallinity. However, modelling and interpreting ultrafast spectroscopy of these systems involves one additional complication: the electron distributions vary in space as well as in time. Within the two temperature model, the spatial variation is usually handled via an electron thermal conductivity term, but this description is only valid over length scales much larger than the characteristic mean free path on the order of tens of nanometers. At intermediate dimensions, super-diffusive and ballistic electron transport effects become important.

On the other extreme, in plasmonic nanoparticles with dimensions on the order of these mean free paths and smaller, the carrier distributions remain spatially homogeneous to an excellent approximation. We therefore pick such plasmonic particles for a first joint experimental and *ab initio* study. Neglecting the spatial dependence allows us to treat the time dynamics and spectral response in much greater detail with electronic structure methods, than previously possible with empirical free-electron models.

Extending such an analysis to the case with spatial transport is the subject of future work. This requires adding spatial degrees of freedom to the Boltzmann equation, and computing the *ab initio* collision integrals as we do here, separately for different points in space. This level of theory will naturally capture super-diffusive / ballistic transport as well as energy-dependence of the carrier mean free paths. Although the theoretical formulation to include spatial dependence is straightforward, the computational expense increases substantially, requiring development of appropriate algorithms to make such calculations practical.

ELECTRON-PHONON COLLISION INTEGRAL

Here we calculate the electron-phonon collision integral for the interaction of an arbitrary hot electron distribution, $f(\varepsilon)$, with a thermal phonon distribution $n(\omega, T_l)$, given by the Bose distribution at lattice temperature T_l. We start with the rate of energy transfer between the electrons and lattice per unit volume, which is exactly (6) and (7) from Ref. 1, except that we allow $f(\varepsilon)$ to be an arbitrary distribution (instead of restricting it to a Fermi distribution at some temperature T_e),

$$\left.\frac{dE}{dt}\right|_{\text{e-ph}} = \frac{2\pi}{\hbar}\int_{BZ}\frac{\Omega d\mathbf{k} d\mathbf{k}'}{(2\pi)^6}\sum_{n'n\alpha}\delta(\varepsilon_{\mathbf{k}'n'}-\varepsilon_{\mathbf{k}n}-\hbar\omega_{\mathbf{k}'-\mathbf{k},\alpha}) \times \hbar\omega_{\mathbf{k}'-\mathbf{k},\alpha}\left|g^{\mathbf{k}'-\mathbf{k},\alpha}_{\mathbf{k}n,\mathbf{k}'n'}\right|^2 S(\varepsilon_{\mathbf{k}n},\varepsilon_{\mathbf{k}'n'},\omega_{\mathbf{k}'-\mathbf{k},\alpha}) \quad (1)$$

with

$$S(\varepsilon,\varepsilon',\omega) \equiv f(\varepsilon)n(\omega)(1-f(\varepsilon'))-(1-f(\varepsilon))(1+n(\omega))f(\varepsilon'). \quad (2)$$

Here Ω is the unit cell volume, $\varepsilon_{\mathbf{k}n}$ is the energy of electron with wave-vector $\mathbf{k}$ in band n, $\hbar\omega_{\mathbf{k}'-\mathbf{k},\alpha}$ is the energy of a phonon with wave-vector $\mathbf{q}=\mathbf{k}'-\mathbf{k}$ and polarization index α, and $g^{\mathbf{k}'-\mathbf{k},\alpha}_{\mathbf{k}'n',\mathbf{k}n}$ is the *ab initio* electron-phonon matrix element coupling this phonon to electronic states indexed by $\mathbf{k}n$ and $\mathbf{k}'n'$. The band index explicitly includes spin as well in order to handle spinorial (relativistic) electronic states, and hence we do not include the conventional spin degeneracy factor present in non-relativistic expressions. (See Ref. 2 for more details.)

The above expressions involve double integrals over the Brillouin zone of *ab initio* electron-phonon matrix elements, and are expensive to evaluate even with the Wannier-function-based formulation that we use,[2] especially if we need to calculate it repeatedly (once per time step) for evaluating the collision integral in the Boltzmann equation. To arrive at a practical approximation which retains electronic structure details, we note that the phonon energy is negligible on the relevant electronic scale ($\hbar\omega \ll \varepsilon, \varepsilon'$). We can then Taylor expand the occupation factors in the energy-conserving cases of $S(\varepsilon,\varepsilon',\omega)$ (which are the only ones that contribute in (1) above) as

$$S(\varepsilon,\varepsilon+\hbar\omega,\omega) \approx -f(\varepsilon)(1-f(\varepsilon)) - \frac{\partial f}{\partial\varepsilon}\hbar\omega[1+n(\omega)-f(\varepsilon)] \quad (3)$$

Further, making the high-temperature phonon occupation factor approximation ($n(\omega) \approx k_B T_l/(\hbar\omega) \gg 1$)

shown to be highly accurate for calculating the total electron-phonon coupling strength in Ref. 3, we can simplify the above expression to

$$S(\varepsilon, \varepsilon + \hbar\omega, \omega) \approx -f(\varepsilon)(1 - f(\varepsilon)) - \frac{\partial f}{\partial \varepsilon} k_B T_l. \quad (4)$$

Now, we can substitute 4 and insert the identity $\int d\varepsilon \delta(\varepsilon - \varepsilon_{\mathbf{k}n})$ into (1), and rearrange it to collect contributions with same initial electron-energy

$$\left.\frac{dE}{dt}\right|_{\text{e-ph}} = -\int d\varepsilon H(\varepsilon) \left[f(\varepsilon)(1 - f(\varepsilon)) + \frac{\partial f}{\partial \varepsilon} k_B T_l \right], \quad (5)$$

with the definition

$$H(\varepsilon) = \frac{2\pi}{\hbar} \int_{BZ} \frac{\Omega d\mathbf{k} d\mathbf{k}'}{(2\pi)^6} \sum_{n'n\alpha} \delta(\varepsilon - \varepsilon_{\mathbf{k}n}) \times \delta(\varepsilon_{\mathbf{k}'n'} - \varepsilon - \hbar\omega_{\mathbf{k}'-\mathbf{k},\alpha}) \hbar\omega_{\mathbf{k}'-\mathbf{k},\alpha} \left| g^{\mathbf{k}'-\mathbf{k},\alpha}_{\mathbf{k}n,\mathbf{k}'n'} \right|^2. \quad (6)$$

Finally, to calculate the electron-phonon contribution to the collision integral $\Gamma_{\text{e-ph}}[f(\varepsilon, t), T_l] = \left.\frac{df(\varepsilon)}{dt}\right|_{\text{e-ph}}$, we note that the contribution to dE/dt from electrons with energy ε corresponds to energy exchange between the lattice and electrons of energy $\varepsilon + \hbar\omega$, where $\hbar\omega$ is negligible on the energy scale of the electrons. Therefore we can equate the energy flow from the electrons to the lattice (the integrand in (5) above) to an energy flow from electrons with energy ε to electrons with energy $\varepsilon + d\varepsilon$, resulting in the differential equation

$$-H(\varepsilon) \left[f(\varepsilon)(1 - f(\varepsilon)) + \frac{\partial f}{\partial \varepsilon} k_B T_l \right] = \frac{\partial}{\partial \varepsilon} \left[g(\varepsilon) \underbrace{\frac{df(\varepsilon)}{dt}}_{\Gamma_{\text{e-ph}}} \right], \quad (7)$$

where $g(\varepsilon)$ is the electronic density of states. Integrating by parts over ε then yields the desired collision integral

$$\Gamma_{\text{e-ph}}[f(\varepsilon), T_l] = \frac{1}{g(\varepsilon)} \frac{\partial}{\partial \varepsilon} \left[H(\varepsilon) \left(f(\varepsilon)(1 - f(\varepsilon)) + \frac{\partial f}{\partial \varepsilon} k_B T_l \right) \right], \quad (8)$$

which is the same as (4) in the main text.

In this approximate form, $H(\varepsilon)$ includes the detailed electronic structure, including energy dependence of the DFT-calculated density of states and electron-phonon matrix elements, but it only needs to be computed once for a material using the computationally-expensive (6). Subsequently, the collision integral given by (8) only involves a single integral over the electron energy which is computationally feasible for efficient solution of the Boltzmann equation. Appendix A presents a numerical tabulation of $H(\varepsilon)$ for the commonly used plasmonic metals, the noble metals and aluminum, which will be useful for implementing this efficient strategy in other analyses of pump probe spectroscopy of plasmonic metals.

Figure 1 plots $H(\varepsilon)$ for the noble metals and aluminum. Note that it varies by over two orders of magnitude with large increases below the Fermi level for noble metals due to d bands, while aluminum exhibits only small variations. The shape of $H(\varepsilon)$ resembles the density of states $g(\varepsilon)$, but it is not strictly proportional to it because the involved electron-phonon matrix elements also vary with energy. We discuss this point at length in Ref. 1, where we plot the quantity $h(\varepsilon) \propto H(\varepsilon)/g(\varepsilon)$.

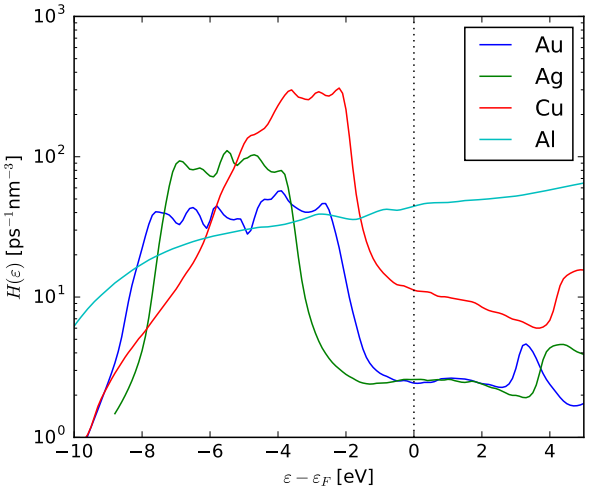

FIG. 1. *Ab initio* calculations of the energy-resolved electron-phonon coupling strength $H(\varepsilon)$ as a function of energy for the noble metals and aluminum, which allows retaining electronic-structure effects in the electron-phonon relaxation at low computational expense. See Appendix A for a numerical tabulation of these functions.

[1] A. M. Brown, R. Sundararaman, P. Narang, W. A. Goddard III, and H. A. Atwater, Phys. Rev. B **94**, 075120 (2016).

[2] A. Brown, R. Sundararaman, P. Narang, W. A. Goddard III, and H. A. Atwater, ACS Nano **10**, 957 (2016).

[3] Z. Lin and L. V. Zhigilei, Physical Review B , 075133 (2008).

Appendix A: Numerical tabulation of $H(\varepsilon)$

$\varepsilon - \varepsilon_F$ [eV]	$H(\varepsilon)$ [ps^{-1}nm^{-3}]			
	Au	Ag	Cu	Al
-10.00	0.597480	0.000000	0.816735	6.198524
-9.90	0.670881	0.000000	0.856266	6.689361
-9.80	0.774425	0.000000	0.902880	7.187018
-9.70	0.898215	0.000000	0.961690	7.703302
-9.60	1.032793	0.000000	1.046594	8.235448
-9.50	1.184179	0.000000	1.189638	8.765580
-9.40	1.363770	0.000000	1.410654	9.294696
-9.30	1.577994	0.000000	1.660172	9.808935
-9.20	1.826637	0.000000	1.890825	10.321572
-9.10	2.113965	0.000000	2.112152	10.842666
-9.00	2.457445	0.000000	2.343315	11.405445
-8.90	2.868770	0.000000	2.598360	12.008095
-8.80	3.386541	1.475556	2.862264	12.595983
-8.70	4.107117	1.618258	3.126024	13.145285
-8.60	5.192705	1.786228	3.413060	13.684712
-8.50	6.908772	1.986710	3.723084	14.266588
-8.40	9.319275	2.230077	4.030691	14.860899
-8.30	12.043378	2.531880	4.331233	15.458478
-8.20	14.865087	2.916826	4.685048	16.055364
-8.10	18.082123	3.427609	5.044037	16.612520
-8.00	22.197636	4.148272	5.371962	17.192309
-7.90	27.323185	5.268445	5.762644	17.790330
-7.80	33.069582	7.184325	6.232967	18.385237
-7.70	38.250519	10.484126	6.730229	18.943394
-7.60	40.531103	15.844491	7.255323	19.462155
-7.50	40.306331	23.601246	7.801365	19.988145
-7.40	39.763118	33.675677	8.411933	20.522898
-7.30	39.405506	46.299891	9.071933	21.033789
-7.20	38.417504	61.757664	9.768299	21.546958
-7.10	36.329505	77.907890	10.523777	22.063230
-7.00	33.787195	88.939596	11.379665	22.524911
-6.90	32.813062	93.446226	12.408457	22.967377
-6.80	35.252292	92.037536	13.606140	23.426765
-6.70	39.545822	86.882304	14.819928	23.907181
-6.60	42.771785	81.543107	16.025767	24.383931
-6.50	43.428595	80.743230	17.459897	24.839701
-6.40	41.676827	81.827254	19.290432	25.273430
-6.30	37.914873	83.165421	21.489945	25.677661
-6.20	33.068636	80.826450	24.210219	26.062922
-6.10	30.885413	76.448005	27.830557	26.463662
-6.00	35.033425	72.838389	32.547644	26.861327
-5.90	42.512403	71.883561	38.280315	27.198252
-5.80	44.670602	76.628940	45.358527	27.488676
-5.70	41.661348	90.777077	52.954444	27.797102
-5.60	38.624055	103.900060	59.872873	28.141901
-5.50	36.820101	110.604850	66.502617	28.477667
-5.40	35.857701	105.218450	73.623761	28.807147
-5.30	35.530336	90.396281	82.379442	29.146016
-5.20	36.110198	86.604494	94.233431	29.483757
-5.10	35.968756	91.477162	108.827669	29.828703
-5.00	31.962004	96.512997	123.718213	30.138029
-4.90	28.101706	98.116865	135.581203	30.396355
-4.80	29.842037	101.840320	141.566473	30.646848
-4.70	36.189737	103.235373	143.726323	30.976934
-4.60	42.932975	101.059671	147.998533	31.302648
-4.50	47.643976	93.836750	153.294295	31.499090
-4.40	49.697666	86.398932	159.238665	31.547582
-4.30	49.433814	81.130231	170.388386	31.643203
-4.20	49.803150	78.124840	188.216701	31.864007
-4.10	52.936707	77.546116	209.783632	32.114375
-4.00	56.637420	78.815377	231.675668	32.376151
-3.90	57.186996	79.820041	253.170326	32.665279
-3.80	53.446850	74.878951	274.375328	33.000097
-3.70	48.705341	60.174976	292.369870	33.438294
-3.60	45.743259	43.903692	299.672044	33.973505
-3.50	43.877397	29.405280	281.384359	34.497851
-3.40	42.289515	19.209973	265.960167	35.001015
-3.30	40.984378	13.209101	262.028505	35.595797
-3.20	40.247768	9.827595	256.885351	36.285612
-3.10	40.237327	7.799188	254.971351	37.029560
-3.00	40.701507	6.471954	266.348686	37.832214
-2.90	41.660842	5.542253	283.624598	38.587687
-2.80	43.653436	4.848347	290.475994	39.005172
-2.70	46.340845	4.331875	283.355087	39.013894
-2.60	46.431320	3.962417	273.305008	38.849016
-2.50	41.809658	3.657115	270.749946	38.551685
-2.40	34.813331	3.412770	279.261668	38.130836
-2.30	28.241631	3.227020	296.272016	37.666112
-2.20	22.429107	3.075512	308.724473	37.184839
-2.10	17.106065	2.935300	283.311241	36.680719
-2.00	12.882255	2.810574	216.920580	36.238897
-1.90	9.923748	2.715421	139.326820	35.893158
-1.80	7.845475	2.638158	83.873314	35.701858
-1.70	6.309495	2.551878	54.253277	35.779615
-1.60	5.119061	2.480718	39.054058	36.231247
-1.50	4.263923	2.439441	30.371743	37.060418
-1.40	3.717504	2.413600	24.933018	37.955130
-1.30	3.380527	2.397134	21.328588	38.833731
-1.20	3.151459	2.404588	18.811727	39.745956
-1.10	2.989413	2.428734	17.076024	40.598065
-1.00	2.863580	2.436585	15.837471	41.359983
-0.90	2.778031	2.437883	14.817745	42.005387
-0.80	2.720992	2.447703	14.017466	42.249750
-0.70	2.648223	2.470743	13.302102	42.020193
-0.60	2.574284	2.493939	12.686451	41.680184
-0.50	2.525533	2.528236	12.257100	41.536025
-0.40	2.523077	2.557014	12.105565	41.832011
-0.30	2.542511	2.585195	12.021962	42.414980
-0.20	2.522894	2.587301	11.740343	43.004344
-0.10	2.470244	2.581560	11.451441	43.693398
0.00	2.435814	2.583180	11.200920	44.425385
0.10	2.426847	2.583427	11.034614	45.085237
0.20	2.436780	2.588506	10.984070	45.737887
0.30	2.464336	2.576051	10.923256	46.300993
0.40	2.463778	2.540278	10.881696	46.642588
0.50	2.464721	2.555209	10.751503	46.838757
0.60	2.495020	2.575880	10.415702	47.001483
0.70	2.559410	2.578451	10.146843	47.058244
0.80	2.614610	2.559763	10.053222	47.040557
0.90	2.623679	2.563904	10.052537	47.077239
1.00	2.630884	2.591037	9.973968	47.203988
1.10	2.642963	2.579932	9.841346	47.458961
1.20	2.634060	2.535060	9.741046	47.693959
1.30	2.620393	2.500295	9.654080	47.965374
1.40	2.620866	2.473010	9.540269	48.386402
1.50	2.604098	2.463454	9.465990	48.708489
1.60	2.577070	2.483351	9.371522	48.851114
1.70	2.543569	2.513114	9.260463	49.012515
1.80	2.496389	2.493051	9.079118	49.208001
1.90	2.450117	2.448111	8.805104	49.394081
2.00	2.416159	2.401856	8.480309	49.578514
2.10	2.396226	2.352809	8.237696	49.799448
2.20	2.383551	2.297894	8.031179	50.062242

$\varepsilon - \varepsilon_F$ [eV]	$H(\varepsilon)$ [ps^{-1}nm^{-3}]			
	Au	Ag	Cu	Al
2.30	2.348383	2.255700	7.898258	50.334948
2.40	2.304990	2.232271	7.810425	50.620405
2.50	2.276492	2.189032	7.704899	50.869306
2.60	2.271009	2.133390	7.566762	51.151426
2.70	2.303656	2.075882	7.378927	51.444578
2.80	2.403414	2.019139	7.153443	51.774267
2.90	2.631845	1.992539	6.967334	52.105309
3.00	3.095318	1.991042	6.871189	52.426393
3.10	3.862063	1.965651	6.784856	52.837046
3.20	4.511806	1.926301	6.650920	53.332478
3.30	4.628620	1.917617	6.459822	53.879606
3.40	4.404569	1.957138	6.255090	54.475118
3.50	4.069953	2.078739	6.106165	55.069544
3.60	3.649925	2.360859	6.008816	55.644777
3.70	3.212520	2.885108	6.009063	56.202618
3.80	2.850649	3.573692	6.112833	56.758981
3.90	2.583920	4.075775	6.350068	57.387389
4.00	2.385781	4.336034	6.838766	58.061439
4.10	2.220298	4.482171	7.942753	58.727943
4.20	2.064424	4.548858	9.876789	59.331686
4.30	1.927370	4.589624	12.049057	59.980713
4.40	1.815514	4.593069	13.493986	60.693005
4.50	1.737646	4.518367	14.244065	61.418616
4.60	1.694126	4.373779	14.762899	62.177836
4.70	1.676210	4.202975	15.175684	62.867071
4.80	1.681104	4.069866	15.490545	63.497082
4.90	1.703042	3.982175	15.635429	64.230583
5.00	1.745026	3.900388	15.587448	64.964196